A. *Structural and technological choices*

The motor that has to be designed is a wheel motor which propels a solar vehicle during a race. The structural and technological choices depend on this situation. Indeed, the materials and the manufacturing costs are not essential while the motor efficiency and the axial bulk are the key points.

Therefore, a brushless DC motor with surface SmCo magnets, concentrated windings, radial flux, and outer rotor [6] is preferred as explained in [7]. An inverter with hysteresis regulated current drives the motor by using the information of three Hall sensors.

B. *Equations for sizing*

Generally, it is easier to start from the geometrical dimensions of a device and to deduce its specifications, such as efficiency and temperature. This is called a *direct model* and requires iterative optimisation techniques to be reversed, i.e. leads to geometrical dimensions when the specifications of the device are known. The non-iterative computation of the geometrical dimensions can be made by using some hypotheses that lead to an *inverse model* which is simpler and suitable for the pre-sizing of the device.

The constitutive analytical equations are non-linear and describe physical phenomena in various fields, e.g. thermal, mechanical, magnetic, and electrical. Their origin is described as well as possible precaution when using them.

1) *Electromechanical conversion*

The expression of the electromagnetic torque C can be obtained from the electromagnetic power given in (1):

$$P_{em}(t) = C(t) \cdot \Omega(t) = \sum_{i=1}^{m} e_i(t) \cdot i_i(t) \qquad (1)$$

where Ω is the rotation speed, m is the number of phases, e_i is the electromotive force (EMF) of phase i, and i_i is the current in phase i. In the case of a brushless DC with three phases and square-wave currents, the EMF is equal to +E during 120 electrical degrees, zero or an indeterminate value during 60 electrical degrees, -E during 120 electrical degrees, and zero or an indeterminate value during 60 electrical degrees. For a wye connection, two phases are on simultaneously and the waveform of the current is as shown in fig. 1 with a peak value equal to +I. Therefore, at constant speed, the electromagnetic power is constant and (1) becomes:

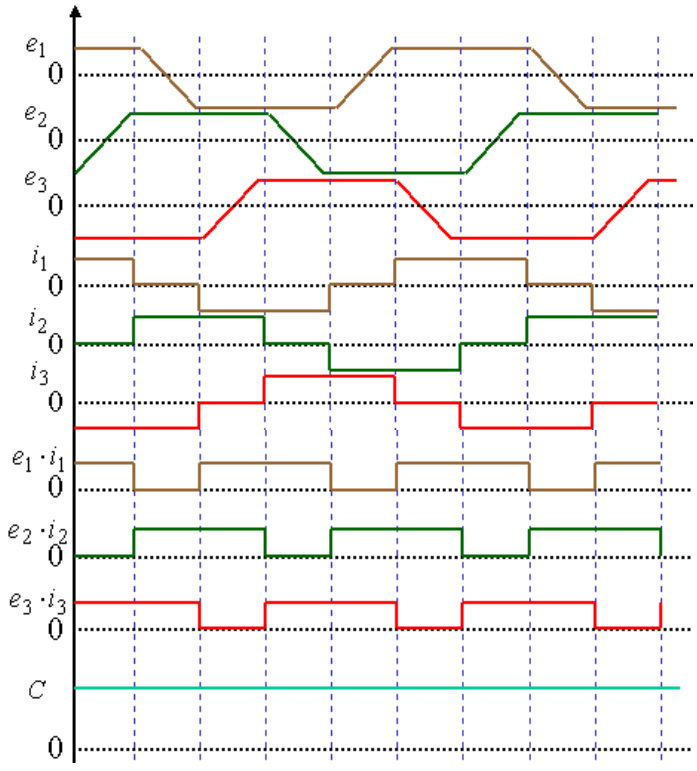

Fig. 1. Electromotive forces, currents, electromagnetic powers for the three phases, and electromagnetic torque resulting. A vertical line is placed all 60 electrical degrees.

$$C \cdot \Omega = 2 \cdot E \cdot I \qquad (2)$$

2) *Lenz's law*

The EMF is computed from the variation of the flux linkage of one coil by using the Lenz's law. When the rotor's displacement is equal to the pole pitch, i.e. π / p , a south magnet takes the place of a north magnet and the flux ϕ reverses, thus:

$$E = \frac{n}{4} \cdot \frac{d\phi}{d\theta} \cdot \frac{d\theta}{dt} = \frac{n}{4} \cdot \frac{2\phi}{\pi/p} \cdot \Omega \qquad (3)$$

where n is the number of supplied conductors, that is the two third of the total number of conductors, and the number of magnets is $2 \cdot p$. The flux ϕ is given when a north magnet is just in front of the coil:

$$\phi = B_e \cdot S_p \qquad (4)$$

where S_p is the surface of a magnetic pole, and B_e is the maximum magnetic induction in the air gap. Equation (3) is built from the hypothesis of a by parts linear variation of the flux versus the rotor position. This gives to a constant by parts EMF. By combining (2), (3) and (4), the electromagnetic torque expression becomes:

$$C = n \cdot I \cdot B_e \cdot \frac{S_e}{2 \cdot \pi} \qquad (5)$$

$$S_e = 2 \cdot p \cdot S_p \qquad (6)$$

where S_e is the total area of the air gap. Equation (5) shows that the electromagnetic torque produced by a brushless DC motor (BLDC) is proportional to the air gap area multiplied by the magnetic induction in the air gap and $n \cdot I$, that is the magnetomotive force (MMF) created by the coils.

For a radial flux BLDC motor, the total air gap area is:

$$S_e = \pi \cdot D_s \cdot L_m \qquad (7)$$

where D_s is the bore (stator) diameter and L_m is the magnetic length of the motor, that is the length of the stack of metal sheets. Equations (3), (4), (6) and (7) lead to :

$$E = \frac{n}{4} \cdot B_e \cdot D_s \cdot L_m \cdot \Omega \qquad (8)$$

A more general approach can be used to give the expression of the electromotive force. Figure 2 presents a simplified view of the magnetic parts in the vicinity of the air gap. Their characteristics condition the EMF waveform. With the hypotheses of a constant air gap thickness and purely radial magnetic induction in the air gap and magnets, the waveform of the magnetic induction in the air gap is as shown in fig. 3. The flux across the coil is computed by integration of the magnetic induction on the area enclosed by the coil borders, defined by the angle α in the cross section. Similarly, the EMF is calculated by derivation of the flux across the coil, giving then the waveforms presented of fig. 4. Let's note that the expression of the EMF is unchanged but that it is now possible to fix the width of the magnets and the opening of the coils so that the flux is maximum, in accordance with (4), and that the plateau of EMF is the largest possible :

$$\alpha = \frac{\pi}{p} \qquad (9)$$

$$\beta = \frac{\pi}{p} \qquad (10)$$

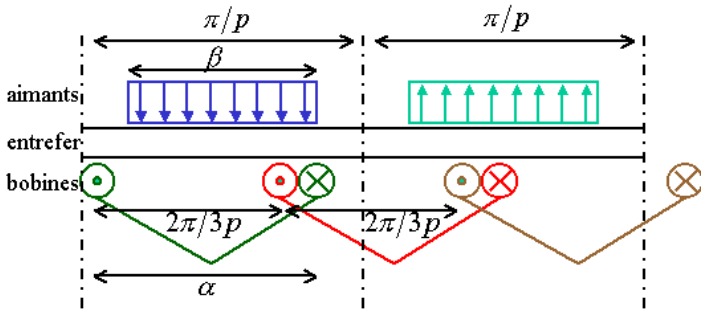

Fig. 2. Vicinity of the air gap, magnets and coils of the stator

FEA have been requested to refine this first analytic approach [8]. An analysis of sensitivity of the width of the plateau of EMF indicated the same tendencies that the analytic approach. However, the variation is non-linear for the parameters α and β. Besides, it has been shown that an intermediate tooth in the middle of every slot was necessary to get a trapezoidal EMF and that the width of its widening α_i has a strong influence. The following relation has been established for a structure with a ratio of the number of slots on the number of magnets equal to 3/4 and assuming that the stator is sufficiently smooth so that the distribution of the induction in the air gap is in conformity with the hypotheses but not too much to avoid to create a magnetic shunt between coils.

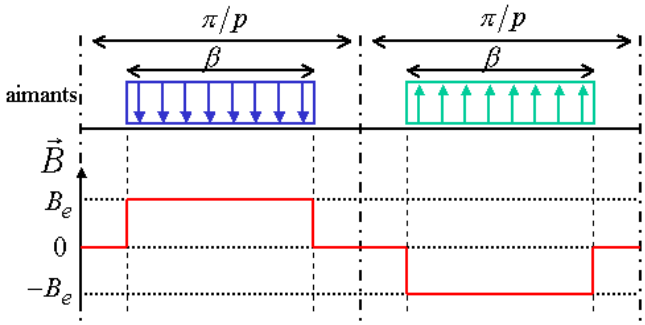

Fig. 3. Magnetic induction waveform in the air gap

$$\alpha_i = \frac{\alpha}{5} \tag{11}$$

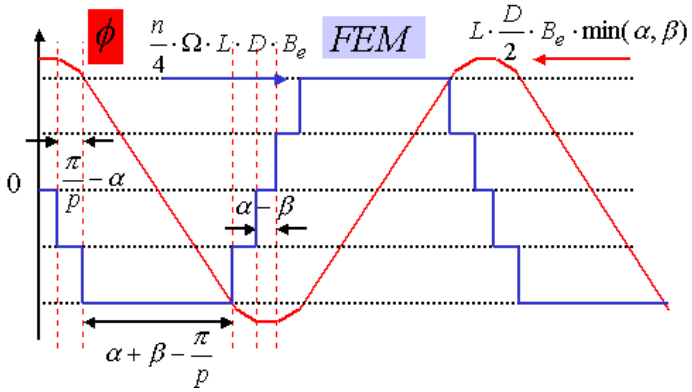

Fig. 4. Flux and electromotive force waveforms

3) Geometrical relations

The main geometric parameters are defined in fig 5. The distances are noted in Latin alphabet and the angles are noted in Greek alphabet. These parameters permit to write several relations of geometric nature:

$$S_{enc} \approx hd \cdot \left[2\pi \cdot \left(\frac{D_s}{2} - eb \right) - \pi \cdot hd - N_e \cdot (li + ld) \right] \tag{12}$$

$$S_{enc} \cdot k_r = \frac{3}{2} \cdot n \cdot \frac{I}{\delta} \tag{13}$$

$$D_{ext} = D_s + 2 \cdot (e + ha + hcr) \tag{14}$$

$$D_{int} = D_s - 2 \cdot (eb + hd + hcs) \tag{15}$$

$$hc = \frac{eb}{\cos(\alpha/2)} - \frac{D_s}{2} \cdot \left(\frac{1}{\cos(\alpha/2)} - 1 \right) \tag{16}$$

$$hi = \frac{D_s}{2} \cdot \left[1 - \cos\left(\frac{\alpha_i}{2} \right) \right] + hc \cdot \cos\left(\frac{\alpha_i}{2} \right) \tag{17}$$

where S_{enc} is the total section of the slots, $k_r < 1$ is the slot filling factor, δ is the current density in the conductors, D_{ext} and D_{int} are the outer and inner diameters, respectively and N_e is the number of slots. The height of hold hc is calculated to get a right angle between the main tooth and the pole shoe. The central thickness of the widening of the intermediate tooth hi is calculated so that the height to the extremity of an intermediate tooth is the same that the one of a main tooth, that is hc, and that there is a right angle between the intermediate tooth and its shoe.

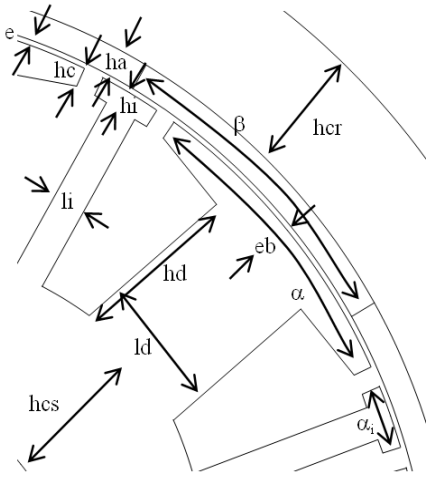

Fig. 5. Geometric parameters of the BLDC motor with radial flux, concentrated winding, permanent magnets and outer rotor

The means radius of a coil end can be approached by:

$$R_{tb} \approx \frac{ld - li}{4} + \left(\frac{D_s}{2} - eb - \frac{hd}{2} \right) \cdot \frac{\pi}{2 \cdot N_e} \qquad (18)$$

The medium length of a half turn is therefore:

$$L_{ds} \approx \frac{L_m}{k_{foi}} + \pi \cdot R_{tb} \qquad (19)$$

where $k_{foi} < 1$ is the bulk factor of the metal sheets.

It is also possible to calculate the total axial length of the motor L_{tot} as well as the masses of the different active parts:

$$L_{tot} \approx \frac{L_m}{k_{foi}} + 2 \cdot \left[\left(\frac{D_s}{2} - eb - \frac{hd}{2} \right) \cdot \frac{\pi}{N_e} - \frac{li}{2} \right] \qquad (20)$$

$$M_a = d_a \cdot p \cdot \beta \cdot ha \cdot \left[ha + 2 \cdot \left(\frac{D_s}{2} + e \right) \right] \cdot L_m \cdot r_{rs} \qquad (21)$$

$$M_{cr} = d_{cr} \cdot \pi \cdot hcr \cdot \left[hcr + 2 \cdot \left(\frac{D_s}{2} + e + ha \right) \right] \cdot L_m \cdot r_{rs} \qquad (22)$$

$$M_{cs} = d_t \cdot \pi \cdot hcs \cdot \left[2 \cdot \left(\frac{D_s}{2} - eb - hd \right) - hcs \right] \cdot L_m \qquad (23)$$

$$M_{ds} \approx d_t \cdot N_e \cdot \left[\begin{array}{l} (ld + li) \cdot hd + \\ \left(\alpha \cdot \dfrac{eb + hc}{2} + \alpha_i \cdot \dfrac{hi + hc}{2} \right) \cdot \dfrac{D_s}{2} \end{array} \right] \cdot L_m \qquad (24)$$

$$M_{cu} = d_{cu} \cdot \frac{3}{2} \cdot n \cdot \frac{I}{\delta} \cdot L_{ds} \qquad (25)$$

$$M_{tot} = M_a + M_{cr} + M_{cs} + M_{ds} + M_{cu} \qquad (26)$$

where M_a, M_{cr}, M_{cs}, M_{ds}, M_{cu}, d_a, d_{cr}, d_t and d_{cu} are the mass and the density of the magnets, the rotor yoke, the stator yoke, the teeth of the stator and the copper, respectively. M_{tot} is the total mass of the active parts and $1.2 \geq r_{rs} \geq 1/k_{foi}$ is the ratio of the length of the rotor on the one of the stator.

4) Flux conservation

The average magnetic induction in the teeth is B_d, B_a in the magnets, B_{cr} in the rotor yoke, and B_{cs} in the stator back iron. Figures 6 and 7 help towards the understanding of the following equations. The conservation of the flux between a main tooth and its widening, named pole shoe, gives:

$$B_d \cdot ld = B_e \cdot \alpha \cdot \frac{D_s}{2} \qquad (27)$$

The same relation applies between an intermediate tooth and its widening:

$$B_d \cdot li = B_e \cdot \alpha_i \cdot \frac{D_s}{2} \tag{28}$$

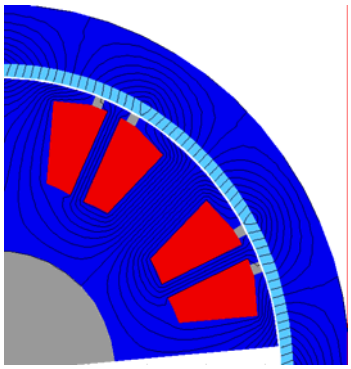

Fig. 6. Magnetic flux in the motor at no-load. A magnet is facing the tooth of the middle.

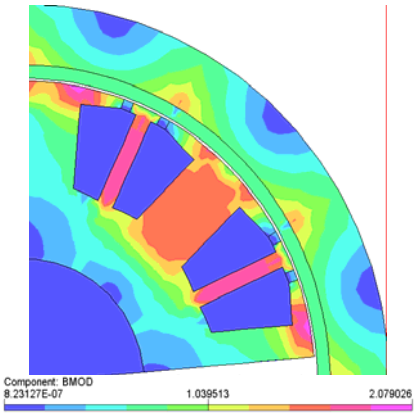

Fig. 7. Magnetic induction (BMOD) in the motor at no-load.

The thickness of the pole shoe is calculated to permit the passage of the flux received by the part of the pole shoe passing the main tooth, so, the flux conservation gives:

$$\begin{aligned} &B_d \cdot \left[eb - \frac{D_s}{2}\left(1 - \cos\left(\sin^{-1}\left(\frac{ld}{D_s}\right)\right)\right)\right] \\ &= B_e \cdot \left[\frac{\alpha}{2} - \sin^{-1}\left(\frac{ld}{D_s}\right)\right] \cdot \frac{D_s}{2} \end{aligned} \tag{29}$$

Half of flux crossing the magnet leaves one side of the rotor yoke whereas other half leaves the other side, thus the conservation of flux between the magnet and the rotor yoke gives:

$$\frac{1}{2} \cdot B_a \cdot \beta \cdot \left(\frac{D_s}{2} + e\right) = B_{cr} \cdot hcr \tag{30}$$

In the same way, the conservation of flux between the main teeth and the stator yoke leads to:

$$\frac{1}{2} \cdot B_d \cdot ld = B_{cs} \cdot hcs \tag{31}$$

Finally, the conservation of the flux between a magnet and a main tooth in conjunction gives:

$$\left[B_a \cdot \beta \cdot \left(\frac{D_s}{2} + e\right) \cdot r_{rs}\right] \cdot k_{fui} = B_e \cdot \alpha \cdot \frac{D_s}{2} \tag{32}$$

where $k_{fui} < 1$ is a leakage coefficient, determined by finite element simulations, that express the fact that the leakage flux between magnets cross the rotor and a part of the air gap but doesn't reach the stator.

5) Ampere's law

It provides a relation between the geometric parameters of the magnets, those of the magnetic circuit, the MMF created by the coils and the magnetic inductions in the different parts.

At no-load, Ampere's law gives:

$$\begin{aligned}&\frac{B_{cr}}{\mu_{cr}(B_{cr})}\cdot\left[\frac{hcr}{2}+\frac{\pi}{2\cdot p}\cdot\left(\frac{D_s}{2}+e+ha+\frac{hcr}{2}\right)\right]\\&+\left(\frac{B_a-B_r(1+\alpha_a\cdot T_a)}{\mu_a}\right)\cdot ha+B_e\cdot e+\frac{B_d}{\mu_t(B_d)}\cdot(eb+hd)\\&+\frac{B_{cs}}{\mu_t(B_{cs})}\cdot\left[\frac{hcs}{2}+\frac{\pi}{N_e}\cdot\left(\frac{D_s}{2}-eb-hd-\frac{hcs}{2}\right)\right]=0\end{aligned}\quad(33)$$

where μ_{cr} and μ_t are the relative magnetic permeabilities of the rotor yoke and sheet metal that depend on the induction level. μ_a, B_r, $\alpha_a<0$ and T_a are respectively the relative permeability, the remnant induction of the magnets to 0°C, its thermal coefficient and the temperature of the magnets.

While supposing that the magnetic permeabilities of the sheet metal and the rotor yoke are more than 1000 times superior to the one of the vacuum and therefore that the MMF consumed in the magnetic circuit is negligible in relation to those consumed in the air gap, (33) simplifies itself by:

$$\left(\frac{B_a-B_r(1+\alpha_a\cdot T_a)}{\mu_a}\right)\cdot ha+B_e\cdot e=0\quad(34)$$

When the motor is in charge, some current circulates in the coils. For an abnormally high current, the magnetic induction in the magnets can reach a critical value provoking a demagnetisation. The induction being then weak, the magnetic permeability is high and it is justified to disregard the MMF consumed in the magnetic circuit. For a critical magnetic induction in the magnets B_c, the phase current takes its admissible peak value and Ampere's law becomes, while exploiting (32):

$$\begin{aligned}&\left(\frac{B_c-B_r(1+\alpha_a\cdot T_a)}{\mu_o\cdot\mu_a}\right)\cdot ha+\frac{n\cdot I_{max}}{4\cdot p}\\&+\frac{B_c}{\mu_o}\cdot\frac{\beta}{\alpha}\cdot\left(1+\frac{2\cdot e}{D_s}\right)\cdot r_{rs}\cdot k_{fui}\cdot e=0\end{aligned}\quad(35)$$

6) Calculation of losses

The resistance of a phase is:

$$R_{ph}=\rho_{cu}\cdot(1+\alpha_{cu}\cdot T_{cu})\cdot\frac{n}{2}\cdot L_{ds}\cdot\frac{\delta}{I}\quad(36)$$

where ρ_{cu} is the resistivity of the copper to 0°C, $\alpha_{cu}>0$ is its thermal coefficient, and T_{cu} is the temperature of the coils. The copper losses are therefore:

$$P_j=2\cdot R_{ph}\cdot I^2\quad(37)$$

The frequency of the fundamental is:

$$f=\frac{p\cdot\Omega}{2\cdot\pi}\quad(38)$$

The iron losses are:

$$P_f=q_t\cdot\left(\frac{f}{f_t}\right)^{1.5}\cdot\left[M_{cs}\cdot\left(\frac{B_{cs}}{B_t}\right)^2+M_{ds}\cdot\left(\frac{B_d}{B_t}\right)^2\right]\quad(39)$$

where q_t represent the specific loss for a frequency f_t and an induction B_t. The efficiency is:

$$\eta=\frac{C\cdot\Omega-P_m}{C\cdot\Omega+P_j+P_f}\quad(40)$$

where P_m are the mechanical losses.

7) Thermal model

The thermal model is very simple. On one hand, it is supposed that the thermal resistances of conduction are always very lower than the thermal resistances of convection. Thus, the temperature is the same in all pieces of the stator in contact, which are the coils, the teeth and the stator yoke.

On the other hand, even though the stator and the rotor are not in contact that by the rolling; big surfaces are face-to-face with a space of air of the order of the tenth of millimetre. In these conditions, the captive air is modelled like a material of weak thermal conductivity. In spite of it, the thermal resistance between rotor and stator is weak since it is equal to the thickness of air divided by the thermal conductivity and the surfaces that are face-to-face. Thus, the gradient of temperature inside the motor is weak and it is supposed that all active materials have the same temperature:

$$T_a = T_{cu} \tag{41}$$

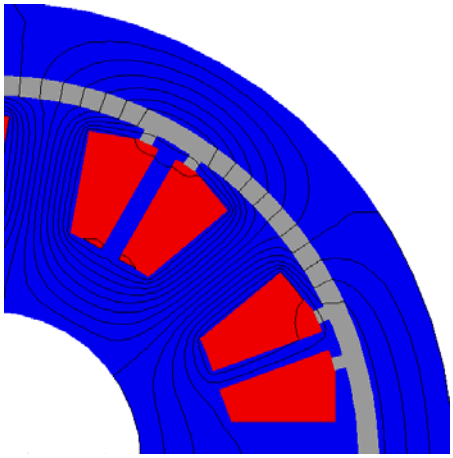

Fig. 8. Flux during a steady rotor FEA, magnets removed.

In the hypothesis of a closed motor, the outside surface of the motor on which occurs the convection is:

$$S_{ext} = \frac{\pi}{2} \cdot D_{ext}^2 + \pi \cdot D_{ext} \cdot L_{tot} \tag{42}$$

The temperature of the motor is therefore:

$$T_{cu} = T_{ext} + \frac{P_j + P_f + P_m}{h \cdot S_{ext}} \tag{43}$$

where h is the coefficient of convection in air and T_{ext} is the temperature of the ambient air.

8) Converter

The knowledge of the inductance of the motor is essential to the survey of the commutations in the phases. Its value is calculated, during a steady rotor simulation, while replacing the magnets by air and while supplying two phases in series (fig. 8). The inductance of phase is given by:

$$L_{ph} \cdot I_{rc} = \psi_{rc} \tag{44}$$

where I_{rc} is the current during this steady rotor trial and ψ_{rc} is the total flux, seen by the phase, produced by this current. It decomposes in a radial flux that crosses the air gap ψ_{ent} and tangent fluxes in the slots ψ_{enc} and in the pole shoe ψ_{bec} (fig. 8):

$$\psi_{rc} = \frac{3}{2} \cdot \psi_{ent} + 2 \cdot (\psi_{enc} + \psi_{bec}) \tag{45}$$

The coefficient 3/2 permits to take into account the mutual fluxes with the other phases whereas the coefficient 2 indicates that the slots and pole shoes surrounding the tooth are crossed by the same leakage flux.

By using Ampere's law, it can be found that the magnetic induction in a rectangular slot is expressed with:

$$B_{enc}(x) = \mu_o \cdot \frac{n_{enc} \cdot I_{rc}}{l_{enc}} \cdot \frac{x}{h_{enc}} \tag{46}$$

where l_{enc} is the width of the slot, h_{enc} is the height of the slot, n_{enc} is the number of conductors in the slots, and x is the distance from the bottom of the slot, at the opposite of the air gap. Therefore, the flux crossing a rectangular slot is:

$$\psi_{enc} = \mu_o \cdot \frac{n_{enc}^2 \cdot I_{rc}}{l_{enc}} \cdot \frac{L_m \cdot h_{enc}}{3} \qquad (47)$$

Using the parameters of the motor, the flux per current unit expresses as:

$$\frac{\psi_{enc}}{I_{rc}} = \mu_o \cdot \frac{1}{16} \frac{n^2}{N_e} \cdot \frac{L_m \cdot hd}{\left(\frac{D_s}{2} - eb - \frac{hd}{2}\right) \cdot \frac{\pi}{N_e} - \frac{ld + li}{2}} \qquad (48)$$

Ampere's law gives the flux per current unit across the air gap and the pole shoe:

$$\frac{\psi_{ent}}{I_{rc}} = \mu_o \cdot \frac{3}{16} \frac{n^2}{N_e} \cdot \frac{L_m}{e + ha} \cdot \alpha \cdot \frac{D_s}{2} \qquad (49)$$

$$\frac{\phi_{bec}}{I_{rc}} = \mu_o \cdot \frac{3}{16} \frac{n^2}{N_e} \cdot \frac{L_m \cdot hc}{\left(\frac{D_s}{2} - \frac{hc}{2}\right) \cdot \left(\frac{\pi}{N_e} - \frac{\alpha + \alpha_i}{2}\right)} \qquad (50)$$

Equations (44) and (45) give:

$$L_{ph} = \frac{3}{2} \cdot \frac{\psi_{ent}}{I_{rc}} + 2 \cdot \left(\frac{\psi_{enc}}{I_{rc}} + \frac{\psi_{bec}}{I_{rc}}\right) \qquad (51)$$

Only the relations (48) to (51) will be used during the sizing for the calculation of the inductance in which the current I_{rc} disappears.

The converter's role is to supply the phases of the motor as shown in fig. 1. All 60 electric degrees, a commutation occurs. In the one drawn in fig. 9 to 11, the current of the phase 3 goes from $+I$ to 0 whereas the one of the phase 1 goes from 0 to $+I$ and the one of the phase 2 maintains itself to $-I$.

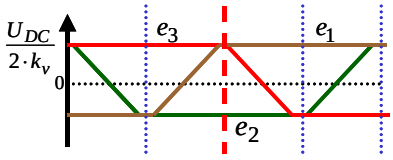

Fig. 9. State of the electromotive forces during the commutation

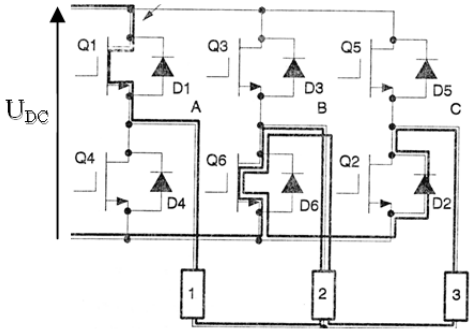

Fig. 10. Currents in the phases during the commutation

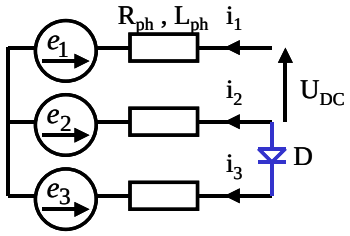

Fig. 11. Simplified circuit during the commutation

Kirchhoff's laws (fig. 11) give:

$$U_{DC} = R_{ph} \cdot i_1 + L_{ph} \cdot \frac{d\, i_1}{d\, t} + e_1 - R_{ph} \cdot i_2 - L_{ph} \cdot \frac{d\, i_2}{d\, t} + e_2 \quad (52)$$

$$0 = R_{ph} \cdot i_2 + L_{ph} \cdot \frac{d\, i_2}{d\, t} + e_2 - R_{ph} \cdot i_3 - L_{ph} \cdot \frac{d\, i_3}{d\, t} + e_3 \quad (53)$$

$$i_1 + i_2 + i_3 = 0 \quad (54)$$

where U_{DC} is the voltage of the DC bus. The electromotive forces during the commutation (in the middle of fig. 9) are:

$$e_1 = e_3 = -e_2 = \frac{U_{DC}}{2 \cdot k_v} = E \quad (55)$$

where $k_v > 1$ is the ratio between the half of the voltage of the DC bus and the electromotive force at the rated speed. Thus, the current in phase 1 is governed by the following differential equation:

$$R_{ph} \cdot i_1 + L_{ph} \frac{d\, i_1}{d\, t} = \frac{U_{DC}}{3} \cdot \left(2 - \frac{1}{k_v} \right) \quad (56)$$

Its expression is therefore:

$$i_1(t) = \frac{U_{DC}}{3 \cdot R_{ph}} \cdot \left(2 - \frac{1}{k_v} \right) \left[1 - \exp\left(- \frac{R_{ph}}{L_{ph}} t \right) \right] \quad (57)$$

The current reaches its peak value to the time:

$$t_1 = - \frac{L_{ph}}{R_{ph}} \cdot \ln \left[1 - \frac{3 \cdot R_{ph} \cdot I}{U_{DC} \cdot (2 - 1/k_v)} \right] \quad (58)$$

In the same way, the expression of the current in phase 3 is:

$$i_3(t) = I\exp\left(-\frac{R_{ph}}{L_{ph}}t\right) - \frac{U_{DC}}{3\cdot R_{ph}}\left(1+\frac{1}{k_v}\right)\left[1-\exp\left(-\frac{R_{ph}}{L_{ph}}t\right)\right] \quad (59)$$

It appears that the current in phase 3 decreases with a slop different of that of the growth of the current in the phase 1. Thus, according to the speed of the motor and the coefficient k_v, the current in phase 2 won't be constant and will present a hollow or a peak. In the sizing process only the equations (55) and (58) will be used to verify that the rise time of the current is reasonable.

The coefficient k_v has a direct influence on the maximal speed of the motor at no-load Ω_{max} :

$$\Omega_{max} = \Omega\cdot\frac{U_{DC}}{2\cdot E} \quad (60)$$

With (55), (60) becomes:

$$\Omega_{max} = k_v\cdot\Omega \quad (61)$$

Only (55), (58), and (61) are used in the sizing program.

9) Material properties

The known material properties are: $k_r = 0.5$, $B_r = 1.045\,T$, $B_c = 0.05\,T$, $\alpha_a = -5\cdot10^{-4}\,K^{-1}$, $\mu_a = 1.05$, $\mu_o = 4\cdot\pi\cdot10^{-7}\,T\cdot m\cdot A^{-1}$, $\rho_{cu} = 1.72\cdot10^{-8}\,ohm\cdot m$, $\alpha_{cu} = 3.8\cdot10^{-3}\,K^{-1}$, $d_t = 7850\,kg\cdot m^{-3}$, $d_a = 7400\,kg\cdot m^{-3}$, $d_{cu} = 8950\,kg\cdot m^{-3}$, $d_{cr} = 7850\,kg\cdot m^{-3}$, $q_t = 2.5\,W\cdot kg^{-1}$, $f_t = 50\,Hz$, $B_t = 1.5\,T$, $h = 10\,W\cdot m^{-2}\cdot K^{-1}$, $T_{ext} = 50\,°C$, and $k_{foi} = 0.95$.

The structure is characterized by the following relation between the number of slots and the number of magnets: $N_e = \frac{3}{2}\cdot p$. The mechanical losses are estimated to $P_m = 15\,W$. Finally, the leakage flux coefficient is identified by FEA: $k_{fui} = 0.8$.

10) Specifications

The specifications give the nominal torque as well as the rated speed: $C = 20\,N.m$ and $\Omega = 721\cdot\pi/30\ rad.s^{-1}$. The maximal speed reached at no-load is specified also $\Omega_{max} = 1442\cdot\pi/30\ rad\cdot s^{-1}$.

II. Results of the Sizing

The input parameters have the following values: $D_s = 189\,mm$, $B_e = 0.75\,T$, $\delta = 3\,A/mm^2$, $B_d = 1.8\,T$, $B_{cs} = 0.8\,T$, $L_m = 45\,mm$, $r_{rs} = 1.11$, $e = 0.8\,mm$, $U_{DC} = 120\,V$, $B_{cr} = 1.2\,T$ et $p = 6$. The unknowns are calculated then from data of the specifications, the material properties and the sizing equations. The results are given in the order of resolution: $\alpha = 30°$, $\beta = 30°$, $\alpha_i = 6°$, $k_v = 2$, $I = 25.168\,A$, $n = 249.162$, $li = 4.123\,mm$, $ld = 20.617\,mm$, $eb = 6.569\,mm$, $hcs = 23.194\,mm$, $Ba = 0.838\,T$, $hcr = 17.413\,mm$, $S_{enc} = 6271\,mm^2$, $hd = 24.934\,mm$, $D_{int} = 79.607\,mm$, $f = 72.1\,Hz$, $hc = 3.467\,mm$, $hi = 3.591\,mm$, $R_{tb} = 17.294\,mm$, $L_{ds} = 101.7\,mm$, $L_{tot} = 95.929\,mm$, $M_{cs} = 2.646\,kg$, $M_{ds} = 2.862\,kg$, and $P_f = 21.096\,W$. This resolution is sequential.

The 7 equations solved simultaneously give: $T_a = T_{cu} = 102.4°C$, $ha = 4.091\,mm$, $D_{ext} = 233.608\,mm$, $R_{ph} = 36\,m\Omega$, $P_j = 45.713\,W$, $S_{ext} = 0.156\,m^2$.

The continuation of the calculations is sequential: $I_{max} = 278.44\,A$, $M_a = 0.925\,kg$, $M_{cr} = 4.637\,kg$, $M_{cu} = 2.854\,kg$, $M_{tot} = 13.924\,kg$, $\eta = 94.812\,\%$, $\psi_{enc}/I_{rc} = 4.351\cdot10^{-5}\,Wb/A$, $\psi_{ent}/I_{rc} = 7.399\cdot10^{-4}\,Wb/A$, $\psi_{bec}/I_{rc} = 7.83\cdot10^{-5}\,Wb/A$, $L_{ph} = 1.353\,mH$, and $t_1 = 0.572\,ms$.